ICLASS 2009,11th International Annual Conference on Liquid Atomization and Spray Sysytems, Vail, Colorado USA, July 2009

Nonlinear Instability and Encapsulation of a Compound Liquid Jet

Takao Yoshinaga*
Department of Mechanical Science, Osaka University,
Osaka 560-8531, Japan

Abstract

We analytically examine the breakup and encapsulation phenomena of a gas-cored compound liquid jet which consists of an inviscid and incompressible core gas and surrounding annular liquid. Applying the long wave approximations to both core and annular phases, a set of reduced nonlinear equations is derived for large deformations of the jet. Breakup of the jet is numerically examined in the equations when disturbances are given at a nozzle exit. It is shown that there exist the most dangerous frequency of the disturbances giving the minimum breakup time or length, where the frequency increases as the increase of the core velocity ratio and as the decrease of the Weber number. It is found that the frequency determines not only the shell formation period but also the produced shell size which is obtained through the volume conservation between the produced shell and one wave length of the disturbance with the dangerous frequency. These formation periods and sizes of the shells well agree with the results in the previous experiment and phenomenological model.

Introduction

A gas or liquid-cored annular jet, which is called a compound jet, is of great importance in various engineering and industrial applications such as coating, encapsulation and atomization techniques [1,2]. It has been experimentally shown that the jet breaks up by sealing-off or ballooning of the annular phase and finally the core phase is encapsulated by the annular one [3,4]. In particular, for a gas-cored liquid jet emanating from an annular nozzle, Kendall [4] observed that a train of liquid shells is naturally produced and its formation frequencies depend upon velocity ratios of the core to the annular phases. Although such frequencies were partially predicted by Lee and Wang [5,6] in their phenomenological model, their analysis was based on a thin annular liquid sheet without a core flow. They examined the instability of the sheet closing at one end under a variable core gas pressure. However, it is expected that the encapsulation is affected large by rapid changes of the local pressure and flow velocity at the bottle neck of the core phase near the breakup. Therefore, the core fluid motion, even for a gas, is essential not only for the breakup but also for the encapsulation or capsule formation. In this paper, the capsule formation process in a gas-cored compound liquid jet is considered from the viewpoint of nonlinear instability. In the analysis, we numerically examine spatial and temporal evolutions of the nonlinear equations derived under the long wave approximations for both core and annular phases. As a result of this, we show that the present analysis can predict well the shell formation frequencies and produced shell sizes.

Formulation

Figure 1 shows the schematic of the jet in the (r, z) axisymmetric coordinate system. Denoting the core and annular phases by subscripts $j = 1$ and 2, respectively, the velocity components are denoted by (v_j, u_j), densities by ρ_j and pressures by p_j. The surfaces are given by $r = h_j$ and the surface tension of the interfaces by σ_j, while the surrounding ambient gas has the constant pressure p_3 and its density is ignored. The thickness of the annular jet b $(= h_2 - h_1)$ and the radius of the mid-plane R $(= (h_2 + h_1)/2)$ are introduced. In the analysis, we assume that the core and annular liquids are inviscid and incompressible, and the gravitational force is negligible.

*Takao Yoshinaga, yoshinaga@me.es.osaka-u.ac.jp

The basic equations are given by the continuity and momentum equations for the core phase ($j = 1$, $0 < r < h_1$) and for the annular phase ($j = 2$, $h_1 < r < h_2$)

$$\nabla \cdot \boldsymbol{u}_j = 0, \tag{1}$$

$$\frac{\partial \boldsymbol{u}_j}{\partial t} + (\boldsymbol{u}_j \cdot \nabla)\boldsymbol{u}_j = -\frac{1}{\rho_j}\nabla p_j, \tag{2}$$

where $\boldsymbol{u}_j = (u_j, v_j)$.

On the other hand, the boundary conditions are given by the kinematic and dynamical conditions on $r = h_1$ and h_2:

$$\text{On } r = h_1 : \frac{\partial h_1}{\partial t} = v_j - u_j \frac{\partial h_1}{\partial z}, \quad p_1 = p_2 + \sigma_1 \kappa_1, \tag{3a}$$

$$\text{On } r = h_2 : \frac{\partial h_2}{\partial t} = v_2 - u_2 \frac{\partial h_2}{\partial z}, \quad p_2 = p_3 + \sigma_2 \kappa_2, \tag{3b}$$

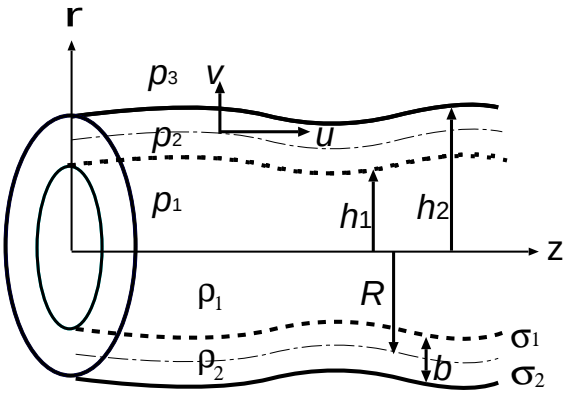

Figure 1: Schematic of the compound liquid jet.

where the curvatures κ_j are given as

$$\kappa_j = h_j^{-1}\left[1 + (\partial h_j/\partial z)^2\right]^{-1/2} - (\partial^2 h_j/\partial z^2)\left[1 + (\partial h_j/\partial z)^2\right]^{-3/2}.$$

The basic equations and the boundary conditions can be simplified by using the long wave approximation in which sufficiently long waves are considered compared with the core radius and annular sheet thickness. In the present analysis, we apply the approximations with different expansion parameters to the core and the annular phases. We assume the variables to be expanded in terms of r^2 for the core phase, while in terms of $r - R$ for the annular phase

$$\begin{aligned}
u_1 &= u_1^{(0)} + r^2 u_1^{(2)} + \cdots, \quad p_1 = p_1^{(0)} + r^2 p_1^{(2)} + \cdots. \\
u_2 &= u_2^{(0)} + u_2^{(1)}(r - R) + u_2^{(2)}(r - R)^2 + \cdots, \\
v_2 &= v_2^{(0)} + v_2^{(1)}(r - R) + v_2^{(2)}(r - R)^2 + \cdots, \\
p_2 &= p_2^{(0)} + p_2^{(1)}(r - R) + p_2^{(2)}(r - R)^2 + \cdots,
\end{aligned} \tag{4}$$

where the coefficients are the functions of z and t.

Using the above expansions into the basic equations and the boundary conditions and neglecting the higher order terms than $O(h_1)$ and $O(b)$, we finally obtain the following reduced equations for b, R, u_1, u_2, v_2 in the lowest order of the approximation:

$$\frac{\partial b}{\partial t} = -\frac{\partial (b u_2)}{\partial z} - \frac{b v_2}{R}, \tag{5a}$$

$$\frac{\partial R}{\partial t} = v_2 - u_2 \frac{\partial R}{\partial z}, \tag{5b}$$

$$\frac{\partial u_1}{\partial t} = -u_1 \frac{\partial u_1}{\partial z} - \frac{1}{\rho}\frac{\partial p_1}{\partial z}, \tag{5c}$$

$$\frac{\partial u_2}{\partial t} = -u_2 \frac{\partial u_2}{\partial z} - \left(\frac{\partial P}{\partial z} - \frac{\Delta P}{b}\frac{\partial R}{\partial z}\right), \tag{5d}$$

$$\frac{\partial v_2}{\partial t} = -u_2 \frac{\partial v_2}{\partial z} - \frac{\Delta P}{b}, \tag{5e}$$

together with the equation for p_1

$$A_1\frac{\partial^2 p_1}{\partial z^2}+A_2\frac{\partial p_1}{\partial z}+A_3 p_1+A_4=0, \tag{5f}$$

where superscripts on the variables have been omitted. In the above representation (5f) the coefficients A_1 to A_4 are the functions of b, R, u_1, u_2, v_2, while

$$P=\frac{1}{2}\left(p_1+p_3\right)-\frac{1}{2\,\mathrm{Wb}}\left(\sigma\kappa_1-\kappa_2\right), \quad \Delta P=-(p_1-p_3)+\frac{1}{\mathrm{Wb}}\left(\sigma\kappa_1+\kappa_2\right),$$

are, respectively, such as the mean pressure of p_1 and p_3 and the pressure difference when the surface tension is taken into consideration. The above set of equations are normalized in terms of the characteristic length H, velocity U, time H/U and pressure $\rho_2 U^2$, while the non-dimensional parameters $\mathrm{Wb}=\rho_2 HU^2/\sigma_2$, $\rho=\rho_1/\rho_2$ and $\sigma=\sigma_1/\sigma_2$ are introduced.

Consequently, the problem can be reduced to solving the above simplified nonlinear equations. In particular, since for an infinitely long jet in the steady state the radius and flow velocity take constant values, we can set $h_1=\bar{h}_1$, $h_2=\bar{h}_2$, $u_1=\bar{u}_1$, $u_2=\bar{u}_2$, $\bar{v}_1=\bar{v}_2=0$. For this case, we have $\Delta P=0$, from which p_1 is found to be always larger than p_3 due to the surface tension

$$\bar{p}_1=p_3+\frac{1}{\mathrm{Wb}}\left(\frac{\sigma}{\bar{R}-\bar{b}/2}+\frac{1}{\bar{R}+\bar{b}/2}\right), \tag{6}$$

where $\bar{R}=(\bar{h}_1+\bar{h}_2)/2$ and $\bar{b}=\bar{h}_2-\bar{h}_1$. In the next, we are going to numerically examine an initial-boundary value problem for disturbances superimposed on the above steady state.

Numerical Results

Kendall [4] showed in his experiment that there exist typical three flow geometries of produced liquid shell depending upon the velocity ratio of the core to the annular ($\bar{u}_1/\bar{u}_2$). For the low velocity ratio ($\bar{u}_1/\bar{u}_2=1.4$), the period length of the produced shells is so long that any adjacent shells are interconnected by a thin liquid thread, while for the high velocity ratio ($\bar{u}_1/\bar{u}_2=12.6$) the period length is too short to separate any adjacent shells which are partially merged. For the medium velocity ratio ($\bar{u}_1/\bar{u}_2=4.2$), however, the shells formed near the nozzle are well separated with each other one after another.

In order to compare with such experimental results, we perform the numerical analysis for the same parameters as in the experiment; $\rho=0.001$, $\sigma=1$, $\bar{h}_2=1$, $\bar{h}_1=0.625$, $\mathrm{Wb}=32.5$. The initial-boundary condition are set for $z=0, t\geq 0$ in such a way that $u_1=\bar{u}_1+\eta\sin(\omega t+\phi)$ and the other variables are given in the steady state such as $\bar{u}_2=1, \bar{v}_1=\bar{v}_2=0$, where the phase ϕ are taken as 0 or π to avoid any velocity jump of u_1. In the calculations, once $\bar{u}_1/\bar{u}_2$, η and ϕ are given, we examine for various ω the breakup time t_b (or the breakup length z_b) that is defined as a time (or length) when the core radius reduces to zero (or regarded as 0). As a result, we can determine the most dangerous frequency ω that gives the shortest t_b or z_b for a given η and ϕ, which means that the frequency can bring about the most unstable breakup in the sense of nonlinear.

Figure 2 shows the breakup profiles for such a ω when $\eta=0.005$ and $\phi=0,\pi$ in three typical cases of the velocity ratios as in the experiment, where we note that z_b is not always smaller for $\phi=\pi$. As is seen from the figure, the annular jet is not yet perfectly closed even at t_b, whose tendency is more enhanced as the velocity ratio increases. This is because the core radius diminishes more rapidly near the breakup as the velocity ratio increases and, therefore, the perfect closing of the annular phase can not be captured within the present numerical resolution, though the zero-core radius becomes singular in the analysis. Nonetheless, since the error in t_b for such a rapid motion may be negligible, we can say, at least, that both t_b and z_b simultaneously decrease as the velocity ratio increases for both ϕ. Such a tendency is in agreement with the experimental observations that the breakup appears more and more near the nozzle exit or in a smaller time when the velocity ratio increases.

(a) $\bar{u}_1/\bar{u}_2 = 1.4$:

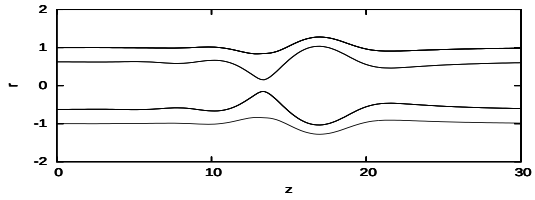

$\omega = 0.9$ $(\phi = 0, t_b = 16.41, z_b = 16.0)$

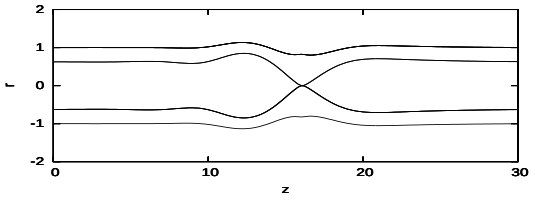

$\omega = 1.06$ $(\phi = \pi, t_b = 17.00, z_b = 13.4)$

(b)$\bar{u}_1/\bar{u}_2 = 4.2$:

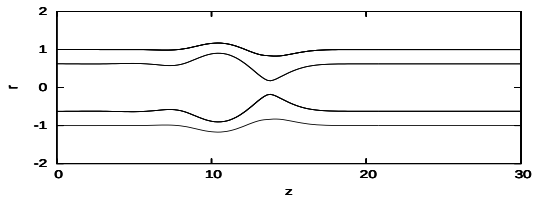

$\omega = 1.03$ $(\phi = 0, t_b = 13.68, z_b = 13.8)$

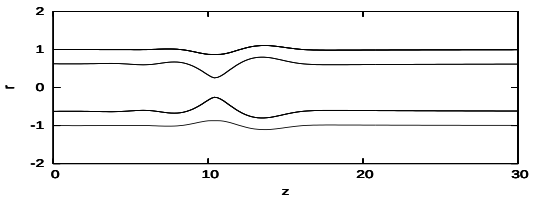

$\omega = 1.31$ $(\phi = \pi, t_b = 13.18, z_b = 10.4)$

(c) $\bar{u}_1/\bar{u}_2 = 12.6$:

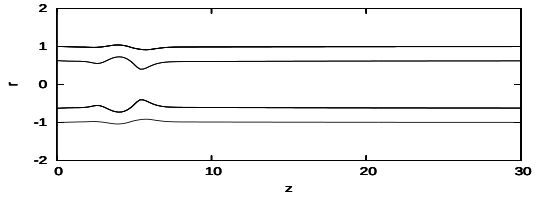

$\omega = 2.11$ $(\phi = 0, t_b = 5.69, z_b = 5.4)$

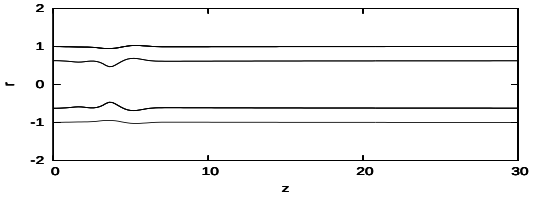

$\omega = 2.61$ $(\phi = \pi, t_b = 5.23, z_b = 3.6)$

Figure 2: Breakup profiles for different velocity ratios.

Since the experiment shows that the shells are naturally produced with a period depending upon the velocity ratio, we expect that the disturbance with a particular frequency out of natural frequencies mainly causes the capsule formation whose period is determined by the particular frequency. We assert that this frequency is nothing but the most unstable ω giving a smaller breakup length of those for $\phi = 0$ and π. In order to confirm this, the numerical results are compared in more detail with the results in the experiment [4] and in the phenomenological model [6].

Figure 3 shows the relation between ω and $\bar{u}_1/\bar{u}_2$ when Wb = 26.9 and other variables are left unchanged, where the solid and broken lines denote, respectively, the numerical results when $\eta = 0.05$ and 0.0005, while the open circles ◯ are of the experiment and the open squares □ are of the model. Although ω increases as the increase of $\bar{u}_1/\bar{u}_2$ for all cases, it is found that the experimental results are in better agreement with the numerical one for $\eta = 0.05$ (solid line), while the results based on the pervious model are in agreement with the numerical one for $\eta = 0.0005$ (broken line). Since η is the magnitude of disturbance on the core and ω becomes larger as a whole for larger η, we can say that a larger disturbance on the core increases a shell formation frequency. In fact, the magnitude of the core disturbance in the experiment is larger than that in the previous model for which the core motion has been ignored.

Besides, as is also seen from the comparison of ω between Fig. 2 for Wb = 32.5 and Fig. 3 for Wb = 26.9, it is found that ω for any velocity ratio increases as Wb increases. This means that the

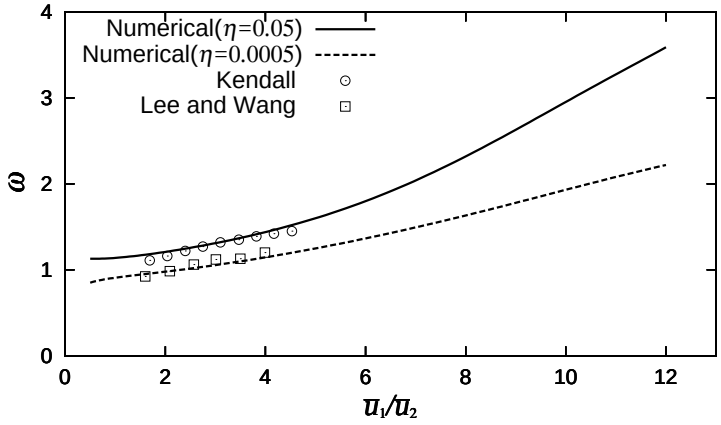

Figure 3: Relation between shell formetion frequencies and core velocity ratios.

shell producing frequency decreases for smaller surface tension or larger Wb, since this shell producing phenomena is based on the surface tension instability. Therefore, it can be said that the most unstable frequency ω determines the shell formation frequency, which increases as the increase of $\bar{u}_1/\bar{u}_2$ and as the decrease of Wb.

Finally, we consider the sizes of the produced shells. Since the shell producing period length λ is given by $\lambda = 2\pi\bar{u}_2/\omega$, the volume of the produced liquid shell may consist of the jet whose length is λ, though the flow velocity difference between the core and the annular should be taken into account. From this volume conservation, the inner and outer radii R_1 and R_2 of the shell are given as

$$\frac{R_2}{\bar{h}_2} = \Big[\frac{3\lambda}{4\bar{h}_2}\big(\frac{\bar{h}_1^2}{\bar{h}_2^2}(\frac{\bar{u}_1}{\bar{u}_2} - 1) + 1\big)\Big]^{(1/3)}, \quad \frac{R_1}{\bar{h}_2} = \Big[(\frac{3\lambda}{4\bar{h}_2})(\frac{\bar{h}_1^2\bar{u}_1}{\bar{h}_2^2\bar{u}_2})\Big]^{(1/3)}. \tag{7}$$

In comparison with the previous results, Fig. 4 shows R_1, R_2 and $\lambda/2$ as functions of $\bar{u}_1/\bar{u}_2$, where the numerical λ, R_1 and R_2 become larger as a whole for smaller η, while these values for both η saturate and approach constant values for sufficiently large velocity ratio. It is also found that the measurements of R_1 and R_2 denoted by ● and ○ and the results of the previous model for R_2 by □ well agree with these numerical results. On the other hand, we note that a half of the shell formation period length should be, at least, larger than the radius of the shell, that is, $\lambda/2 > R_1$. Resulting from this, in order for well separated liquid shells to be produced, we need a smaller velocity ratio than the critical one for which the curves of $\lambda/2$ are across those of the shell radii in Fig. 4. This critical value is estimated to be about 6, which is also confirmed from the fact that the experimental measurements are not obtained for larger values than this ratio.

Conclusions

From the numerical results of the nonlinear evolutions of disturbances on the semi-infinite jet, we obtain the following conclusions: (i) There exists a frequency ω which gives the minimum breakup time t_b (or length z_b) when the disturbances at the nozzle exit are examined for various frequencies. (ii) The frequency increases as the increase of the velocity ratio of the core to the annular and the amplitude of the disturbance, while decreases as the increase of Wb. (iii) The shell formation period and the produced shell radii are well predicted by using this ω and found to be in good agreement with the results of the experiment and the phenomenological model.

The frequency ω is the most dangerous frequency for the breakup of the jet, that is, the most unstable in the sense of nonlinearity. This means that a particular frequency of disturbances can survive during

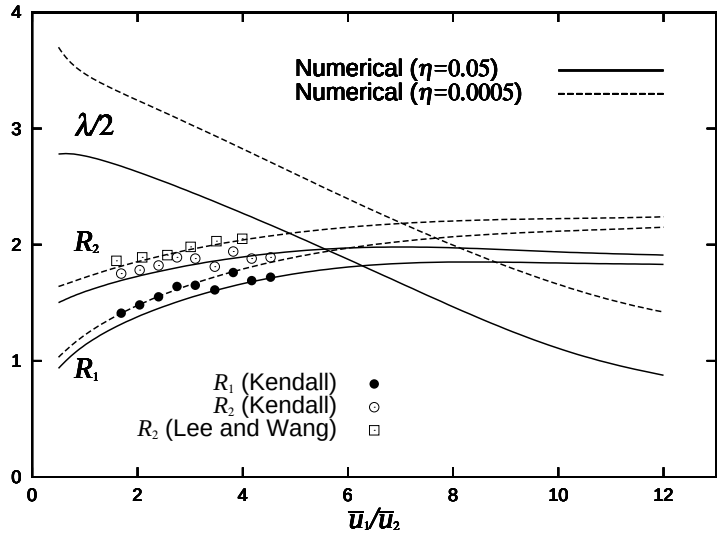

Figure 4: Shell formation period length λ and inner and outer radii R_1, R_2 of the shells for the core velocity ratios.

the breakup process and determines the shell formation period, while the corresponding wavelength of the disturbance may vary in such a process. Consequently, the mechanism of shell formation in the compound liquid jet can be explained by the nonlinear instability.

Acknowledgments

This work has been partially supported by the Grant-in-Aid for Science Research from the Ministry of Education, Culture, Sports, Science and Technology of Japan (No.19560173).

References

1. Lefebvre, A.H., *Atomization and sprays* (Hemisphere, New York, 1989).
2. Lin, S. P., *Breakup of liquid sheets and jets* (Cambridge, 2003) pp.172-200.
3. Hertz, C. H. and Hermanrud, B., "A liquid compound jet," J.FLuid Mech **131**, 271 (1983).
4. Kendall, J. M., "Experiments on annular liquid jet instability and on the formation fo liquid shells," Phys. Fluids, **29**, 2086 (1986).
5. Lee, C. P. and Wang, T. G., "A theoretical model for the annular jet instability," Phys. Fluids **29**, 2076 (1986).
6. Lee, C. P. and Wang, T. G., "A theoretical model for the annular jet instability-Revisited," Phys. Fluids **A 1**, 967 (1989).